Volume 3, Issue 3, 2020 ISSN: 2664-0821
DOI: https://doi.org/10.31058/j.ap.2020.33001

Transmission and Reflection Analysis on Metal/Semiconductor Structure for Quantum Confinement Model by FDTD Technique

May Su Hlaing[1*], Myint Myint Than[1], Tint May Nway[1], Win Kay Khaing[1], Hla Myo Tun[1]

[1] Department of Electronic Engineering, Yangon Technological University, Yangon, Myanmar

Email Address

ecdepartment.ytu@gmail.com (May Su Hlaing)
*Correspondence: ecdepartment.ytu@gmail.com

Received: 25 May 2020; **Accepted:** 2 June 2020; **Published:** 4 June 2020

Abstract:

The paper presents the transmission and reflection analysis on metal-semiconductor structure for quantum confinement model by FDTD technique. The research problem in this study is to understand the transmission and reflection spectrum from the interface of metal and semiconductor combined devices based on the quantum mechanical effect. The objective of this study is to implement the simulation code for quantum mechanics concepts by MATLAB. The analysis on quantum mechanical analysis of the quantum confinement for semiconductor devices which would be designed based on metal-semiconductor structure is numerically investigated in this study. In this paper a macroscopic model was presented, which embraces an innovative approach to equivalent the vertical carrier profile and unites it with a conventional representation in lateral direction firstly. The numerical results prove a momentous enhancement pertaining to the accuracy of the carrier profile and the physical characteristics of the semiconductor devices. The second stage of this study is mainly focused on the transmission and reflection spectrum on the interface of metal/semiconductor structure based on the finite difference time domain techniques.

Keywords:

Quantum Confinement, Device Modelling, FDTD, Numerical Analysis, Quantum Mechanical Analysis

1. Introduction

It is recognized that in significance of the increasingly lessening feature sizes quantum mechanical effects are receiving more imperative for the performance of up to date semiconductor devices. This concern is extensively scrutinized and implicit at physical stage, but a numerical analysis is a long way from inconsequential and numerically very expensive. The state-of-the-art macroscopic models integrating quantum mechanical effects were essentially premeditated to fit the physical characteristics of the investigated semiconductor devices [1,2,3] but not for a completely device modelling. In this paper a fresh move toward to model the quantum confinement near the semiconductor surface is established which does not only equivalent the physical characteristics but also tolerates the device modelling analysis on semiconductor devices and related Semiconductor devices. Moreover the innovative model is proficient to equivalent the vertical carrier profile incredibly precisely, consequently contribution of fresh imminent into the genuine properties of contemporary devices in real world.

The charge carriers in semiconductors afford the beginning for a variation of significant technologies, together with computers, semiconductor lasers, and light emitting devices. The enduring demand to condense the physical size of next-generation electronic devices necessitates progressively smaller building blocks in electronics. Nanostructures with sizes well below 100 nm, such as semiconductor nanocrystals and nanowires, afford such building blocks. Henceforth, it is ostensible that there is both a technological and essential interest in the properties of charge carriers in both bulk and nanostructured materials [4,5,6,7,8].

Quantum mechanics effects based on carrier dynamics considerations are vital role to enhance the fabrication of high performance device structure. The FDTD analyses on reflection and transmission pulses are very essential for numerical analysis [9,10].

The rest of the paper is organized as follows. Section II is pointed out the fundamental concepts of quantum mechanical model for interface engineering. Section III mentions the algorithm of two dimension finite difference time domain (2D FDTD) algorithm for the numerical analysis between metal and semiconductor interface. Section IV presents the simulation results of numerical analysis. Section V expresses the discussions on simulation results and conclusion of this study.

2. Quantum Mechanical Model

The conventional device modelling pilots to two important inaccuracies pertaining to the carrier concentration nears the semiconductor surface. Initial, the dividing of the conduction band into quite a few discrete eigenvalues is not measured. That goes ahead to an over evaluation of the surface charge, as the energy difference between those discrete eigenvalues and the Fermi-level is superior than the one from the bottom of the conduction band to the Fermi-level. Next, the conventional models do not regard as that the shape of the wave functions diminishes the carrier concentration near the Semiconductor surface as well. Therefore, a meticulous approach to imitate the carrier concentration has to make sure of both effects, by contributing the rough calculation for the wave function and the actual band structure of Semiconductor Devices.

2.1. Approach to Wave Function Approximation

The first of Quantum Mechanical effects by a diminution of the density of states SD near the Semiconductor interface affecting an exponential shape function called Wave Function Approximation. This pursues an approach proposed by [9].

$$SD(i)=SD\left(1-e^{-(i-i_0)^2/\lambda_{Thermal}}\right) \tag{1}$$

where 'i' is the distance to the Semiconductor interface and 'i0' is an offset to match the nonzero carrier concentration near the surface stanching from the finite barrier height. λThermal is the thermal wavelength conscientious for the lessening of the Quantum Mechanical effects with increasing distance from the Semiconductor interface,

$$\lambda_{Thermal}=\frac{\sqrt{2mkT}}{\hbar} \quad (2)$$

If that improvement is utilized the qualitative carrier distribution near the Semiconductor interface in physically powerful inversion is duplicated quite well, but devoid of deliberation of band structure effects, this is not the issue in the threshold level region [10].

2.2. Approach to Energy Band Structure Approximation

Figure 1 illustrates the conduction band energy near the surface of a semiconductor device, intended with a self-consistent Schrödinger-Poisson model working with the effective mass come up to Quantum Mechanical Model [10]. Near the surface the lowest eigenenergy is connotation higher than the band edge, thus reasoning an over evaluation of the charge when the conventional imitation approach is utilized. The essential initiative of the current model is to substitute the effective band edge by the first discrete energy level (see Fig. 1). This appears realistic as quantum mechanical computations confirm that regularly more than 95% of the carriers are in that energy band.

The band edge at the Semiconductor surface is set to

$$E^{QMM}_{g,\ Semicon\ Surface}=E^{Conventional}_{g,\ Semicon\ Surface}+\Delta E_g \quad (3)$$

whereas $E^{QMM}_{g,\ Semicon\ Surface}$ is the developed bandgap energy which is utilized in the Boltzmann statistics, $E^{Conventional}_{g,\ Semicon\ Surface}$ is the bandgap in accordance with the material specification, and ΔE_g is the applied modification. The current model attaches the band edge $E^{QMM}_{g,\ Semicon\ Surface}(i)$ surrounded by the device to the value of $E^{QMM}_{g,\ Semicon\ Surface}$ as long as $E^{QMM}_{g,\ Semicon\ Surface} > E^{Conventional}_{g,\ Semicon\ Surface}$ (i).

As the accurate computation of the first energy level is numerically expensive and necessitates the explanation of the Schrödinger equation and estimation is utilized. The offset ΔE_g is estimated subsequent an establishment of Van Dort et al. [11-14], which reads as

$$\Delta E_g=\frac{13}{9}\beta\left(\frac{\epsilon}{4qkT}\right)^{1/3}|E_{semicon\ surface}|^{2/3} \quad (4)$$

whereas $|E_{semicon\ surface}|$ is the magnitude of the electric field at the semiconductor interface and ϵ is the permittivity of the semiconductor. $\beta = 4.1\times 10^{-8}$ eVcm is an empirical constant.

3. FDTD Algorithm

3.1. Mathematical Expressions of 2D FDTD for Magnetic Fields

The modelling equations for defining the finite difference condition are revealed in this section. Initially, the finite difference equations for H_x, H_y, and H_z for magnetic field expressions are as follows [15].

Volume 3, Issue 3, 2020 ISSN: 2664-0821
DOI: https://doi.org/10.31058/j.ap.2020.33001

$$\frac{E_z^{i,j+1,k}\Big|_t - E_z^{i,j,k}\Big|_t}{\Delta y} - \frac{E_y^{i,j,k+1}\Big|_t - E_y^{i,j,k}\Big|_t}{\Delta z} = -\frac{\mu_{xx}^{i,j,k}}{C_0}\frac{\tilde{H}_x^{i,j,k}\Big|_{t+\frac{\Delta t}{2}} - \tilde{H}_x^{i,j,k}\Big|_{t-\frac{\Delta t}{2}}}{\Delta t} \quad (5)$$

$$\frac{E_x^{i,j,k+1}\Big|_t - E_x^{i,j,k}\Big|_t}{\Delta z} - \frac{E_z^{i+1,j,k}\Big|_t - E_z^{i,j,k}\Big|_t}{\Delta x} = -\frac{\mu_{yy}^{i,j,k}}{C_0}\frac{\tilde{H}_y^{i,j,k}\Big|_{t+\frac{\Delta t}{2}} - \tilde{H}_y^{i,j,k}\Big|_{t-\frac{\Delta t}{2}}}{\Delta t} \quad (6)$$

$$\frac{E_y^{i+1,j,k}\Big|_t - E_y^{i,j,k}\Big|_t}{\Delta x} - \frac{E_x^{i,j+1,k}\Big|_t - E_x^{i,j,k}\Big|_t}{\Delta y} = -\frac{\mu_{zz}^{i,j,k}}{C_0}\frac{\tilde{H}_z^{i,j,k}\Big|_{t+\frac{\Delta t}{2}} - \tilde{H}_z^{i,j,k}\Big|_{t-\frac{\Delta t}{2}}}{\Delta t} \quad (7)$$

3.2. Mathematical Expressions of 2D FDTD for Electric Fields

The additional helping is to catch the electric field expressions founded on E_x, E_y, and E_z from Maxwell's Equations [15].

$$\frac{\tilde{H}_z^{i,j,k}\Big|_t - \tilde{H}_z^{i,j-1,k}\Big|_t}{\Delta y} - \frac{\tilde{H}_y^{i,j,k}\Big|_t - \tilde{H}_y^{i,j,k-1}\Big|_t}{\Delta z} = \frac{\varepsilon_{xx}^{i,j,k}}{C_0}\frac{E_x^{i,j,k}\Big|_{t+\Delta t} - E_x^{i,j,k}\Big|_t}{\Delta t} \quad (8)$$

$$\frac{\tilde{H}_x^{i,j,k}\Big|_t - \tilde{H}_x^{i,j,k-1}\Big|_t}{\Delta z} - \frac{\tilde{H}_z^{i,j,k}\Big|_t - \tilde{H}_z^{i-1,j,k}\Big|_t}{\Delta x} = \frac{\varepsilon_{yy}^{i,j,k}}{C_0}\frac{E_y^{i,j,k}\Big|_{t+\Delta t} - E_y^{i,j,k}\Big|_t}{\Delta t} \quad (9)$$

$$\frac{\tilde{H}_y^{i,j,k}\Big|_t - \tilde{H}_y^{i-1,j,k}\Big|_t}{\Delta x} - \frac{\tilde{H}_x^{i,j,k}\Big|_t - \tilde{H}_x^{i,j-1,k}\Big|_t}{\Delta y} = \frac{\varepsilon_{zz}^{i,j,k}}{C_0}\frac{E_z^{i,j,k}\Big|_{t+\Delta t} - E_z^{i,j,k}\Big|_t}{\Delta t} \quad (10)$$

4. Analyses and Discussions

The representation was realized into the device modelling and numerous characteristic configurations were pretended in order to investigate its device design competences [16]. A potential motivation for the speed up can be the smoother distributions when quantum confinement is taken into consideration.

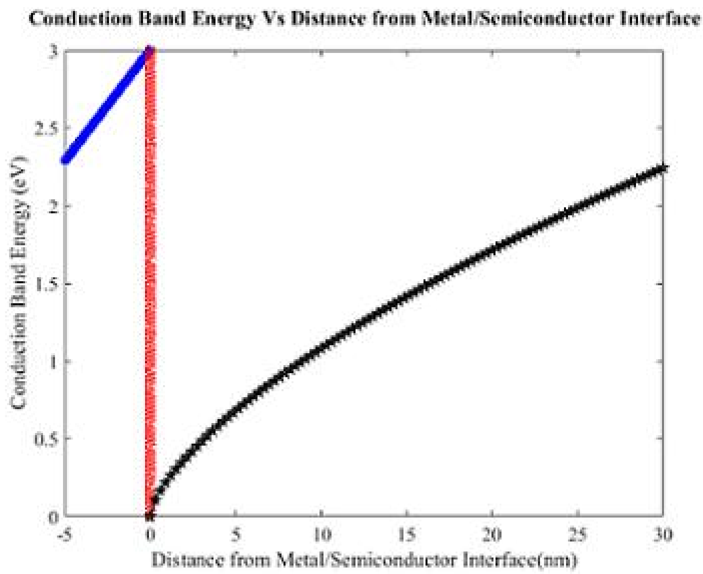

Figure 1. *Conduction Band Energy for Quantum Mechanical Model.*

Figure 2 illustrates the comparison of the Junction Capacitance characteristics obtained with the Quantum Mechanical Model, the Schrödinger-Poisson solver, and the Conventional model. An admirable fit between the results from the Quantum Mechanical Model and the quantum mechanical calculations is achieved; particularly the commencement of inversion is envisaged exceptionally precisely. The over evaluation of the capability in strong inversion is a well-known consequence stalking from the dissimilar allocation statistics applied in the Schrödinger solver (Fermi-Dirac) and the Quantum Mechanical Model.

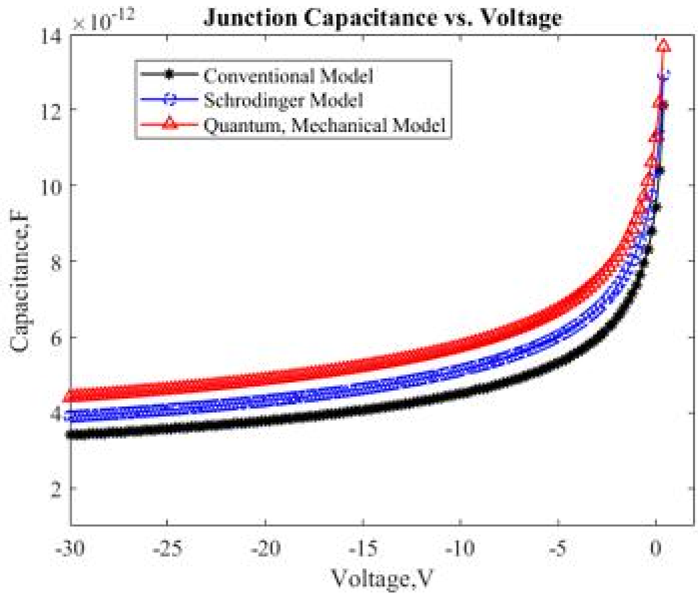

Figure 2. *Junction Capacitance Vs Voltage.*

Figure 3 demonstrates the comparison of electron concentration silhouettes. It can be obviously observed that the Quantum Mechanical Model proffers a straight fit to the results from quantum mechanical calculation. The conventional model contemplates the charge more rapidly to the semiconductor surface, which is a significance of the reasonably smaller band gap. The Quantum Mechanical Model proves the outstanding results with junction capacitance and Electron Concentration according to the numerical investigation.

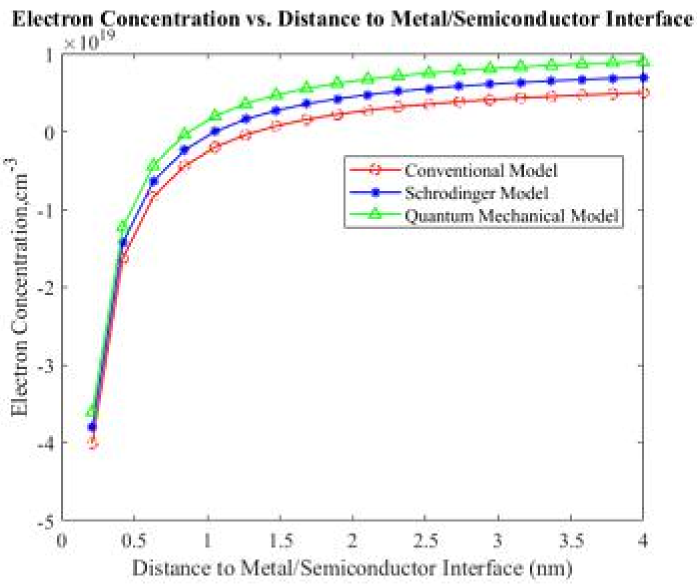

Figure 3. *Electron Concentration Vs Distance to Semiconductor Surface.*

Figure 4 shows the transmission spectrum based on PML boundary. The transmission spectrum starts at the interface of metal/semiconductor interface which was 165 nm. The perfectly match layer boundary is very suitable for considering the transmission spectrum based on FDTD algorithm.

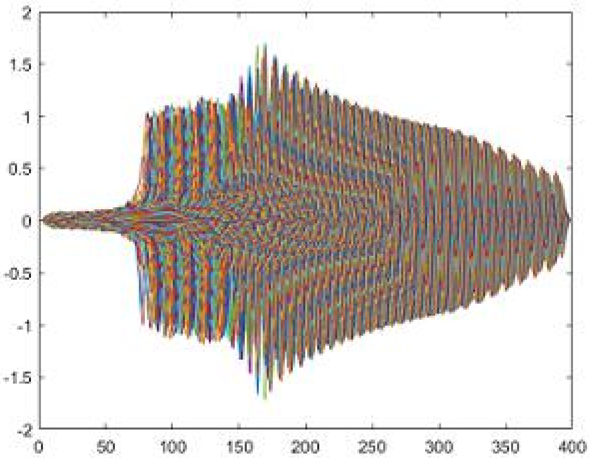

Figure 4. *Transmission Spectrum Based on PML Boundary.*

Figure 5 illustrates the transmission spectrum based on MUR boundary. The transmission spectrum finds at the interface of metal/semiconductor interface which was 185 nm. The Mur absorbing boundary could not be observed the total spectrum for considering the transmission spectrum based on FDTD algorithm.

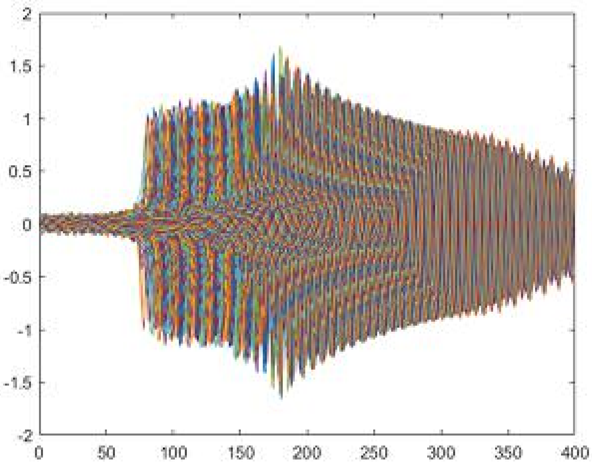

Figure 5. *Transmission Spectrum Based on MUR Boundary.*

Figure 6 demonstrates the reflection spectrum based on PML boundary. The reflection spectrum surprises at the interface of metal/semiconductor interface which was 215 nm. The perfectly match layer boundary is very appropriate for considering the reflection spectrum based on FDTD algorithm.

Figure 7 mentions the reflection spectrum based on MUR boundary. The reflection spectrum finds at the interface of metal/semiconductor interface which was 240 nm. The Mur absorbing boundary could not be detected the total spectrum for considering the reflection spectrum based on FDTD algorithm.

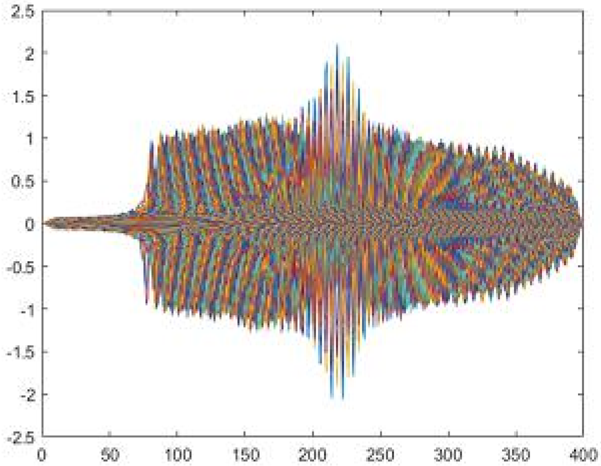

Figure 6. *Reflection Spectrum Based on PML Boundary.*

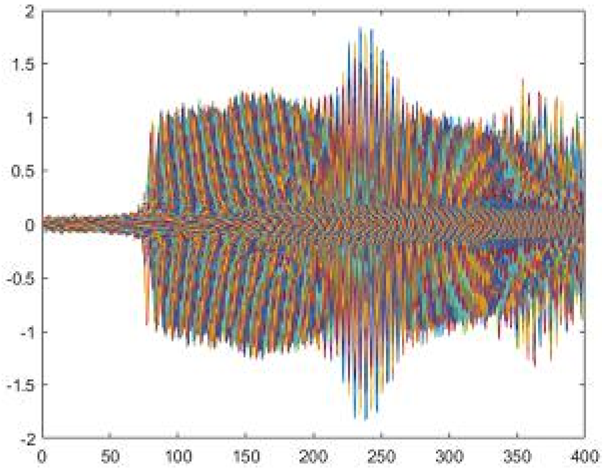

Figure 7. *Reflection Spectrum Based on MUR Boundary.*

5. Conclusions

According to the simulation results on transmission and reflection spectrum based on PML and MUR boundary condition with FDTD algorithm, the PML condition for both transmission and reflection spectrums are very suitable for considering the interace effect with quantum mechanical model for high performance device fabrication. In this paper an innovative comprehensive representation for the simulation of the quantum confinement near the semiconductor surface was presented. An incredibly superior fit was got hold of for the vertical carrier profile and mutually with the excellent physical properties a deeper imminent into the properties of prospect semiconductor devices creations is promising. The conduction band energy for quantum mechanical model proves that the actual device fabrication for semiconductor devices has prominent performance for optical communication purposes.

Conflicts of Interest

The authors declare that there is no conflict of interest regarding the publication of this article.

Author Contributions

This study mainly focuses on the transmission and reflection analysis on metal-semiconductor structure for quantum confinement model by FDTD technique. The theoretical analyses on mathematical modelling for FDTD analysis are vital role to enhance the high performance device fabrication for future semiconductor technology. This work could be provided to find the solution for research problems in advanced modelling techniques for power devices in reality.

Funding

This work is partially supported by Government Research Funds Grant No of GB/D(4)/2019/1.

Acknowledgment

The authors would like to thank many colleagues from the semiconductor research group of the Department of Electronic Engineering from Yangon Technological University.

References

[1] Chow, P. Computer Solutions to the Schrödinger Equation. *Am.J.Phys.,* 1972, 40, 730-734.

[2] Ansch, W.H.; Vogelsang, T.; Kircher, R.; Orlowski, M. Carrier Transport Near the Si/SiO2 Interface of a MOSFET. *Solid-State Electron.,* 1989, 32(10), 839-849, .

[3] Datta, S.; Das, B. Electronic Analog of the Electro-optic Modulator. *Appl. Phys. Lett.,* 1990, 56, 665-667.

[4] Dort, M.V.; Woerlee, P.; Walker, A. A Simple Model for Quantisation Effects in Heavily-Doped Silicon MOSFETs at Inversion Conditions. *Solid-State Electron.,* 1994, 37(3), 411-414.

[5] Hallstein, S.; Berger, J.D.; Hilpert, M.; Schneider, H.C.; Rűhle, W.W.; Jahnke, F.; Koch, S.W.; Gibbs, H.M.; Khitrova, G.; Oestreich. M. Manifestation of Coherent Spin Precession in Stimulated Semiconductor Emission Dynamics. *Phys. Rev. B,* 1997, 56, R7076–R7079.

[6] Yu, Z.; Dutton, R.; Kiehl, R. Circuit/Device Modeling at the Quantum Level. in IWCE-6, Osaka, Japan, 1998; pp. 222-229.

[7] Binder, T.; Dragosits, K.; Grasser, T.; Klima, R.; Knaipp, M.; Kosina, H.; Mlekus, R.; Palankovski, V.; Rottinger, M.; Schrom, G.; Selberherr, S.; Stockinger, M. MINIMOS-NT User's Guide. Institut f˙ur Mikroelektronik, 1998.

[8] Ando, A.; Hasunuma, R.; Maeda, T.; Sakamoto, K.; Miki, K.; Nishioka, Y.; Sakamoto, T. Conducting Atomic Force Microscopy Studies on Local Electrical Properties of Ultrathin SiO_2 Films. *Appl. Surf. Sci.* 2000, 401, 162-163.

[9] Richter, C.A.; Vogel, E.M.; Hodeg, A.M.; Hefner, A.R. Differences Between Quantum-Mechanical Capacitance-Voltage Simulators. in Simulation of Semiconductor Processes and Devices, (Athens, Greece), Sept. 2001.

[10] Holub, M.; Shin, J.; Chakrabarti, S.; Bhattacharya, P. Electrically Injected Spin-Polarized Vertical-Cavity Surface-Emitting Lasers. *Appl. Phys. Lett.* 2005, 87, 091108.

[11] Chang, S.J.; Jhou, Y.D.; Lin, Y.C.; Wu, S.L.; Chen, C.H.; Wen, T.C.; Wu, L.W. GaN-based Metal-Semiconductor-Metal Photodetectors Fabricated on Patterned Sapphire Substrates. *IEEE Photonics Technology Letters,* 2008, 20(22), 1866-1868, DOI: 10.1109/LPT.2008.2004814.

[12] Taniyama, T.; Wada, E.; Itoh, M.; Yamaguchi, M. Electrical and Optical Spin Injection in Ferromagnet/Semiconductor Heterostructures. *NPG Asia Mater,* 2011, 3, 65-73.

[13] Wang, G.S.; Lu, H.; Chen, D.J.; Ren, F.F.; Zhang, R.; Zheng, Y.D. High Quantum Efficiency GaN-based p-i-n Ultraviloet Photodetectors Prepared on Patterned Sapphire Substrates. *IEEE Photonics Technology Letters,* 2013, 25(7).

[14] Jia, R. et al. Polarization Enhanced Charge Transfer: Dual-Band GaN-Based Plasmonic Photodetector. *Sci. Rep.,* 2017, 7, 40483, DOI: 10.1038/srep40483.

[15] Phyoe, S.; Kathy, K.M.; Hla, M.T. Zaw Min Naing, Win Khaing Moe. Analysis on Photo Emission and Absorbing Spectrum on GaN Sample by Finite Difference Time Domain Method. *Optics,* 2018, 7(1), 32-37.

[16] Kathy, K.; Phyoe, S.W.; Hla, M.T.; Zaw, M.N.; Win, K.M. Photoluminescence and Lifetime Measurement for the Excitation and Temperature Dependence of Carrier Relaxation in III-V Semiconductors. *Optics,* 2018, 7(1), 38-42, DOI: 10.11648/j.optics.20180701.16.